Supporting Information for:

Nona-coordinated chiral Eu(III) complexes with stereoselective ligand-ligand noncovalent interactions for enhanced circularly polarized luminescence

Takashi Harada,[*,†] *Hiroyuki Tsumatori,*[‡] *Katsura Nishiyama,*[*,†] *Junpei Yuasa,*[‡]

Yasuchika Hasegawa[*,§] *and Tsuyoshi Kawai*[*,‡]

[†] Faculty of Education, Shimane University,

1060 Nishikawatsu-Cho, Matsue, Shimane 690-8504, Japan

[‡] Graduate School of Materials Science, Nara Institute of Science and Technology,

8916-5 Takayama-Cho, Ikoma, Nara 630-0192, Japan

[§] Divisions of Materials Chemistry, Graduate School of Engineering, Hokkaido University,

North-13 West-8, Kita-Ku, Sapporo, Hokkaido 060-8628, Japan

Authors Email Address:

Dr. T. Harada; h-takashi@edu.shimane-u.ac.jp

Prof. T. Kawai; tkawai@ms.naist.jp

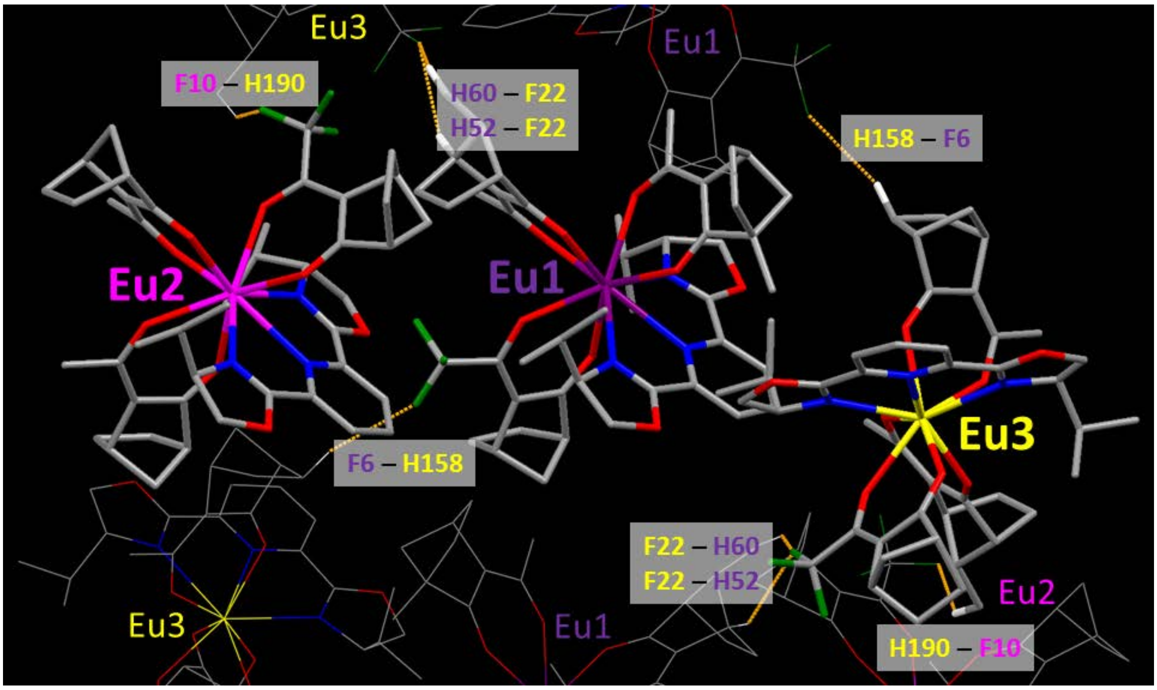

Figure S1. Intermolecular interactions of **1-*R***. Purple atoms; Eu1, pink; Eu2, yellow; Eu3, red; O, blue; N, green; F, gray; C, white; H. Capped sticks represents a minimum unit. Some atoms are omitted for clarity.

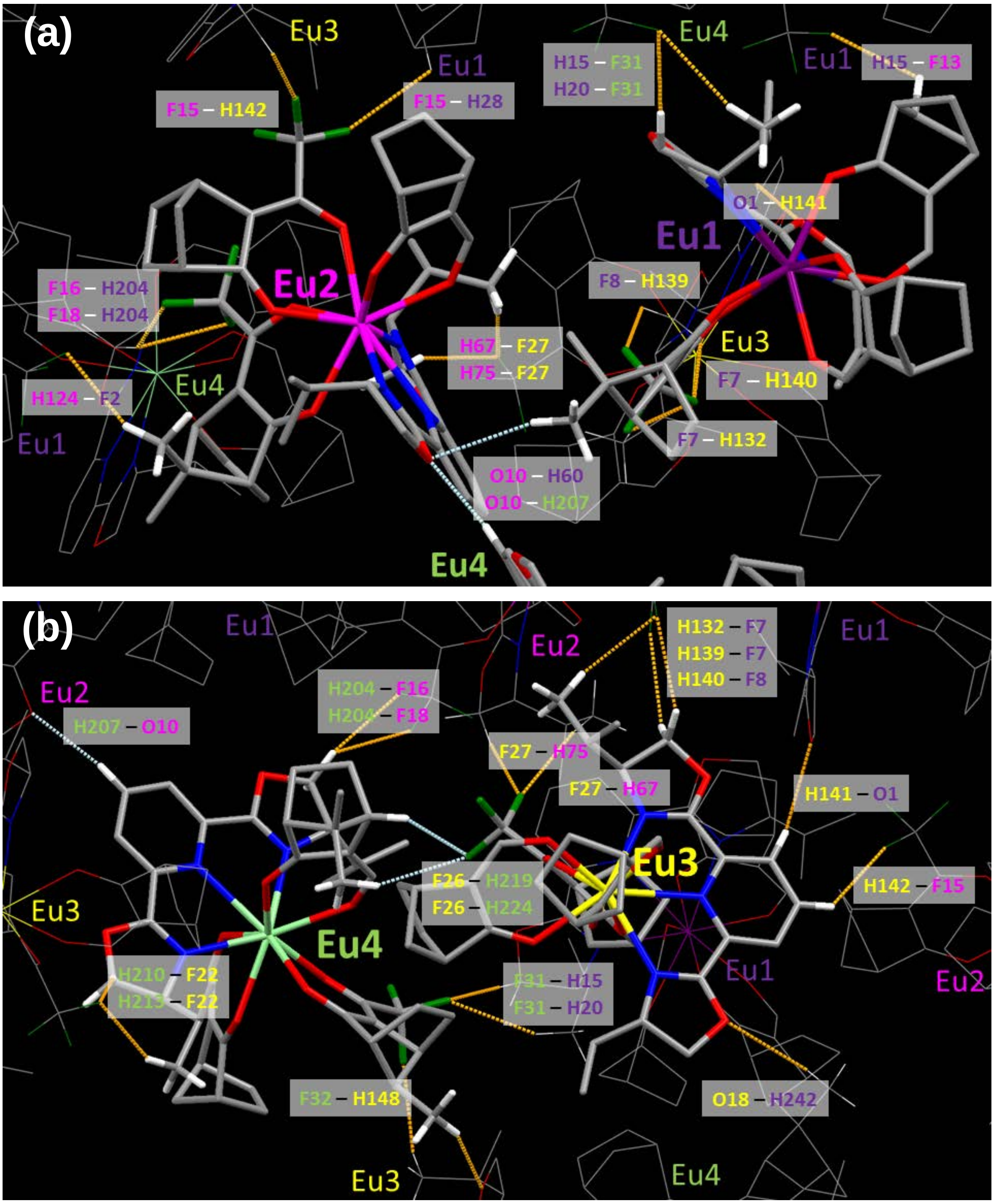

Figure S2. Intermolecular interactions of **1-*S***, (a) around Eu1 and Eu2 and (b) around Eu3 and Eu4 center. Purple atoms; Eu1, pink; Eu2, yellow; Eu3, light green; Eu4, red; O, blue; N, green; F, gray; C, white; H. Capped sticks represents a minimum unit. Some atoms are omitted for clarity.

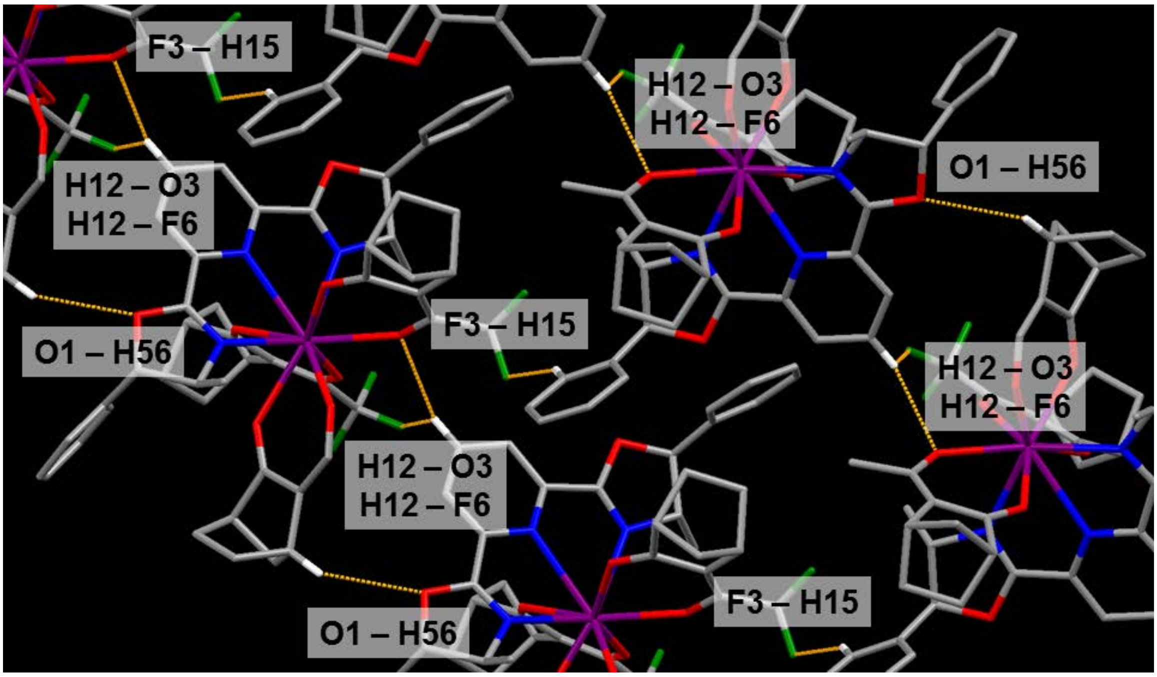

Figure S3. Intermolecular interactions of **2-*SS***. Purple atoms; Eu, red; O, blue; N, green; F, gray; C, white; H. Some atoms are omitted for clarity.

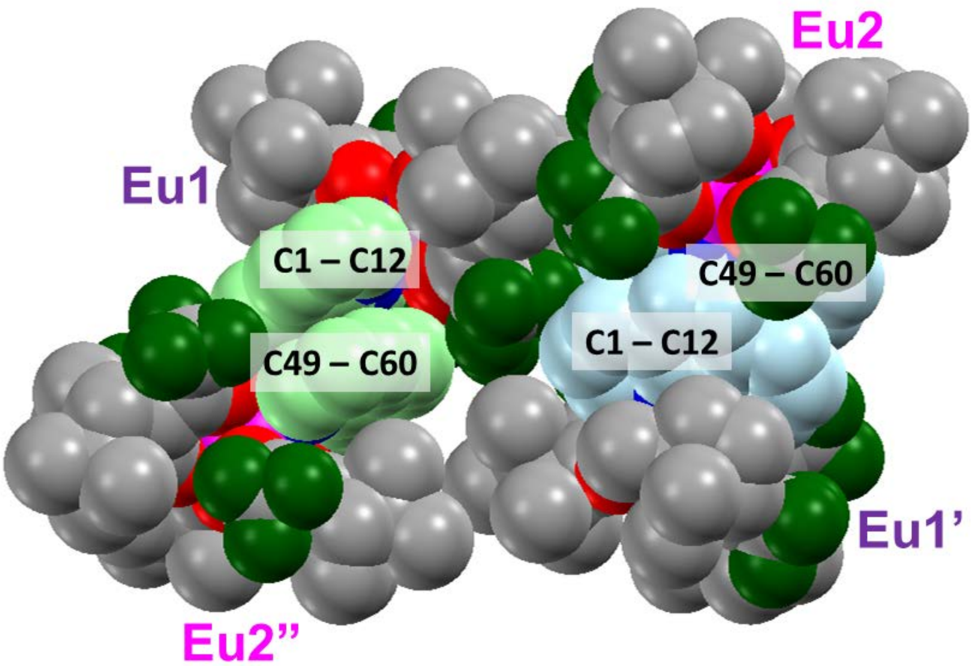

Figure S4. Intermolecular interactions of **3**. Purple atoms; Eu1, pink; Eu2, red; O, blue; N, green; F, gray; C. Light blue and light green represents Phen rings. Some atoms are omitted for clarity. Distance and angles between C1-C12 ring and C49-C60 ring are found to be 3.38 Å and 1.8 degree.

Table S1. Dihedral angles between characteristic planes of *D*-facam ligands in **1-*R***, **1-*S*** and **2-*SS***

complex	plane 1	plane 2	dihedral angles / deg
1-*R*, Eu1 site	*D*-facam1 (O3 and O4)	*D*-facam2 (O5 and O6)	86.1
		D-facam3(O7 and O8)	72.5
	D-facam2	*D*-facam3	77.3
1-*S*, Eu1 site	*D*-facam1	*D*-facam2	66.9
		D-facam3	87.4
	D-facam2	*D*-facam3	66.5
2-*SS*	*D*-facam1	*D*-facam2	27.1
		D-facam3	76.5
	D-facam2	*D*-facam3	74.7

Table S2. Bond lengths and bond angles in Eu(III) Complexes

complex	Eu—O, Eu—N length / Å	N…N, O…O length / Å	N—Eu—N, O—Eu—O angles / deg
1-*R*, Eu1 site	Eu1—N1; 2.57	N1…N2; 2.70	N1—Eu1—N2; 61.9
	Eu1—N2; 2.68	N2…N3; 2.71	N2—Eu1—N3; 61.4
	Eu1—N3; 2.64	O3…O4; 2.88	O3—Eu1—O4; 71.7
	Eu1—O3; 2.49	O5…O6; 2.84	O5—Eu1—O6; 71.8
	Eu1—O4; 2.44	O7…O8; 3.00	O7—Eu1—O8; 79.2
	Eu1—O5; 2.41		
	Eu1—O6; 2.43		
	Eu1—O7; 2.34		
	Eu1—O8; 2.38		
1-*S*, Eu1 site	Eu1—N1; 2.69	N1…N2; 2.75	N1—Eu1—N2; 61.9
	Eu1—N2; 2.67	N2…N3; 2.69	N2—Eu1—N3; 61.5
	Eu1—N3; 2.59	O3…O4; 2.87	O3—Eu1—O4; 72.7
	Eu1—O3; 2.40	O5…O6; 2.98	O5—Eu1—O6; 77.5
	Eu1—O4; 2.44	O7…O8; 2.85	O7—Eu1—O8; 71.8
	Eu1—O5; 2.36		
	Eu1—O6; 2.40		
	Eu1—O7; 2.34		
	Eu1—O8; 2.51		
2-*SS*	Eu1—N1; 2.59	N1…N2; 2.71	N1—Eu1—N2; 61.5
	Eu1—N2; 2.70	N2…N3; 2.71	N2—Eu1—N3; 60.7
	Eu1—N3; 2.66	O3…O4; 2.87	O3—Eu1—O4; 73.7
	Eu1—O3; 2.38	O5…O6; 2.91	O5—Eu1—O6; 74.2
	Eu1—O4; 2.41	O7…O8; 2.81	O7—Eu1—O8; 70.7
	Eu1—O5; 2.40		
	Eu1—O6; 2.43		
	Eu1—O7; 2.37		
	Eu1—O8; 2.48		
3, Eu1 site	Eu1—N1; 2.69	N1…N2; 2.72	N1—Eu1—N2; 62.9
	Eu1—N2; 2.67	O1…O2; 2.81	O1—Eu1—O2; 72.5
	Eu1—O1; 2.40	O3…O4; 2.89	O3—Eu1—O4; 74.7
	Eu1—O2; 2.44	O5…O6; 2.87	O5—Eu1—O6; 74.2
	Eu1—O3; 2.36		
	Eu1—O4; 2.40		
	Eu1—O5; 2.34		
	Eu1—O6; 2.51		

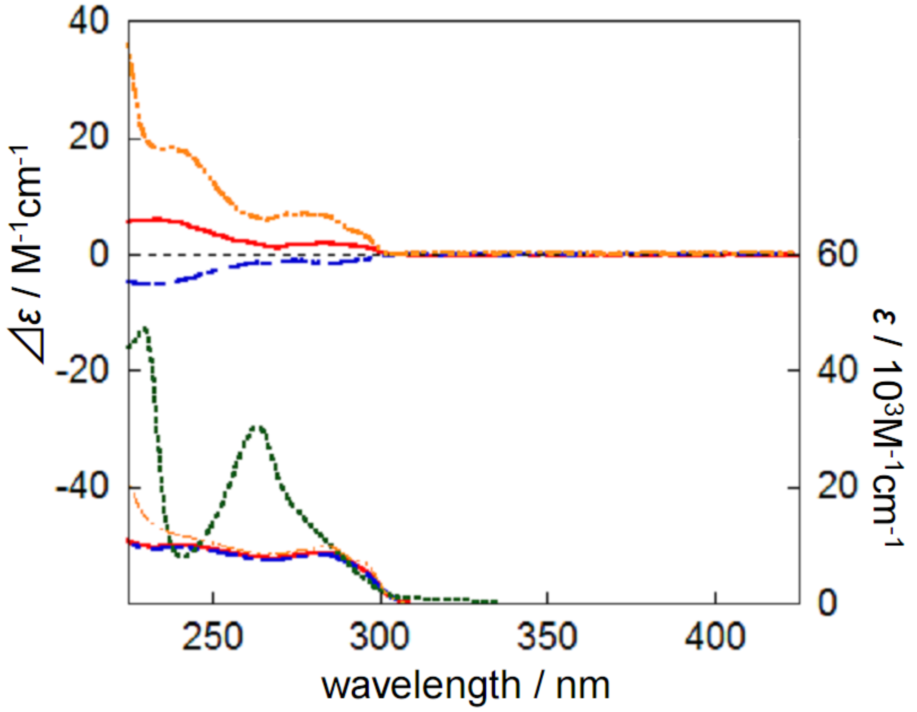

Figure S5. UV-Vis (lower) and CD (upper) spectra of *R*-iPr-Pybox (red line, 12 μM), *S*-iPr-Pybox (blue, 10 μM), *S,S*-Me-Ph-Pybox (orange, 11 μM) and Phen (green, 17 μM) ligands. Solvents used are methanol for *R*-iPr-Pybox, *S*-iPr-Pybox, and Phen, and THF for *S,S*-Me-Ph-Pybox.

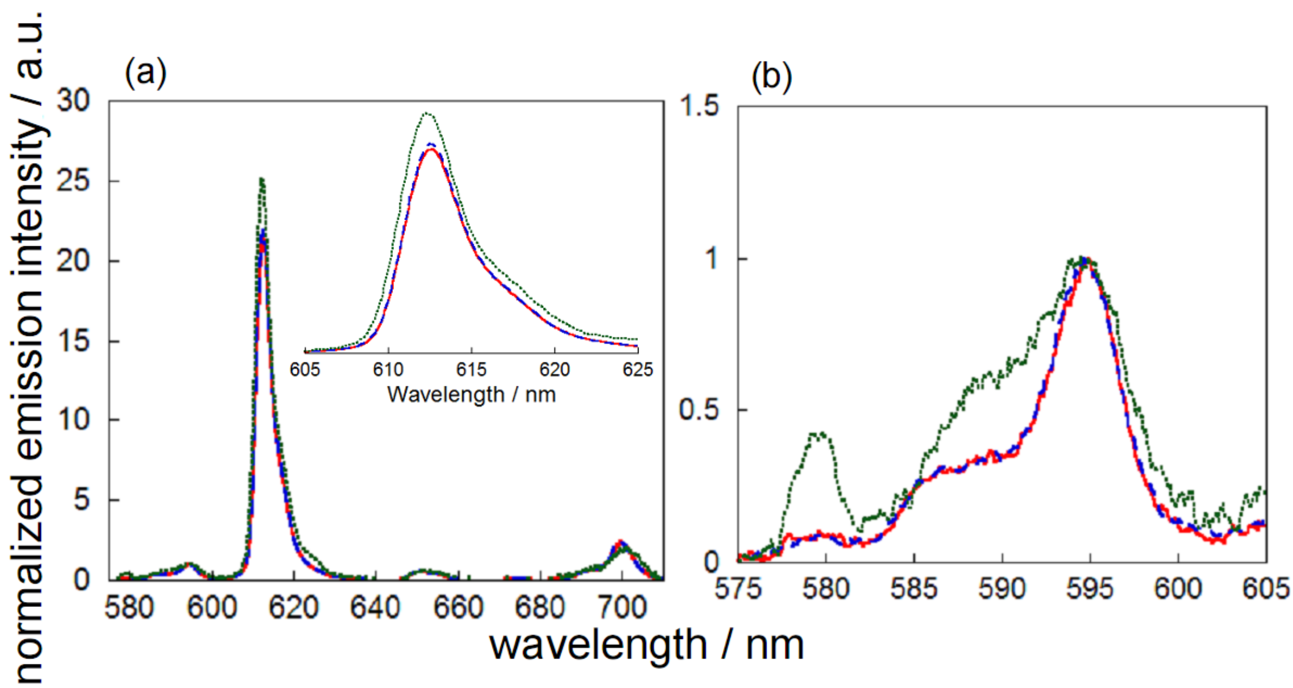

Figure S6. (a)Normalized emission spectra of **1-*R*** (red line), **1-*S*** (blue), and **3** (green), (b) expansion in the wavelength range corresponding to the $^5D_0 \rightarrow {}^7F_0$ and the $^5D_0 \rightarrow {}^7F_1$ transitions. Inset; $^5D_0 \rightarrow {}^7F_2$ transition. Solvents used are acetonitrile-d_3 (1.0 mM). All spectra are normalized at 594 nm.

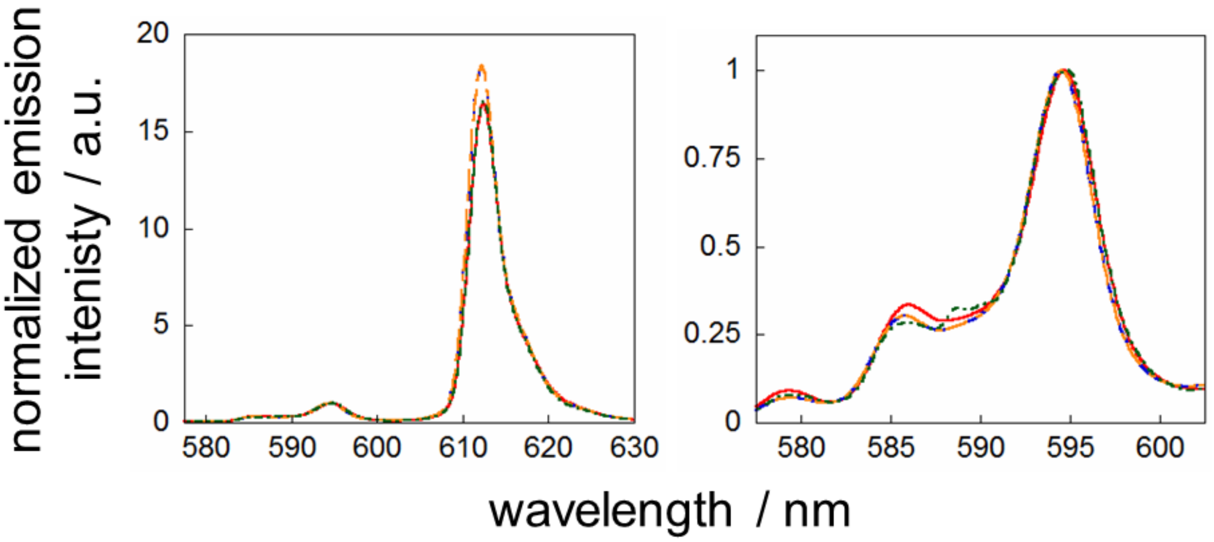

Figure S7. Normalized emission spectra of **1-*R*** (red line, 8.4 μM), **1-*S*** (blue, 13 μM), **2-*SS*** (orange, 25 μM) and **3** (green, 14 μM). Solvents used are acetone-d_6. All spectra are normalized at around 594 nm.

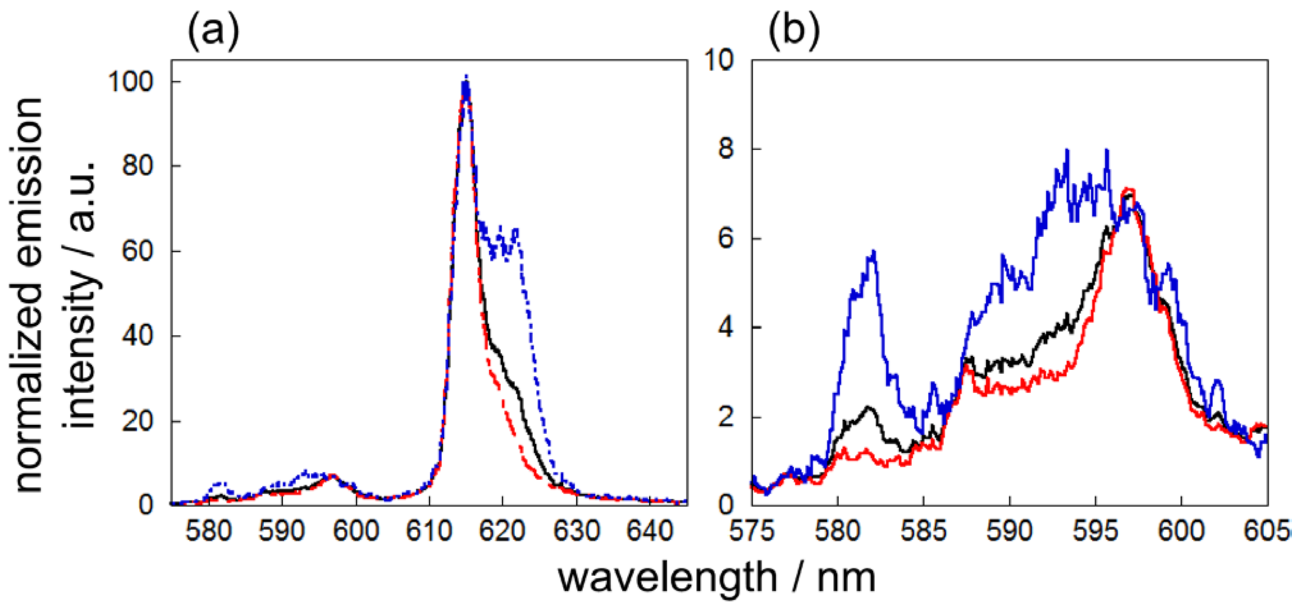

Figure S8. (a) Time evolution of the emission spectra of **2-*SS*** (in acetone-d_6, 1.0 mM). (b) Expansion for $^5D_0 \rightarrow {}^7F_0$ and the $^5D_0 \rightarrow {}^7F_1$ transitions. 0.0−2000 μs (black line), 0.0−250 μs (blue), and 250−2000 μs (red). These spectra were normalized at 615 nm.

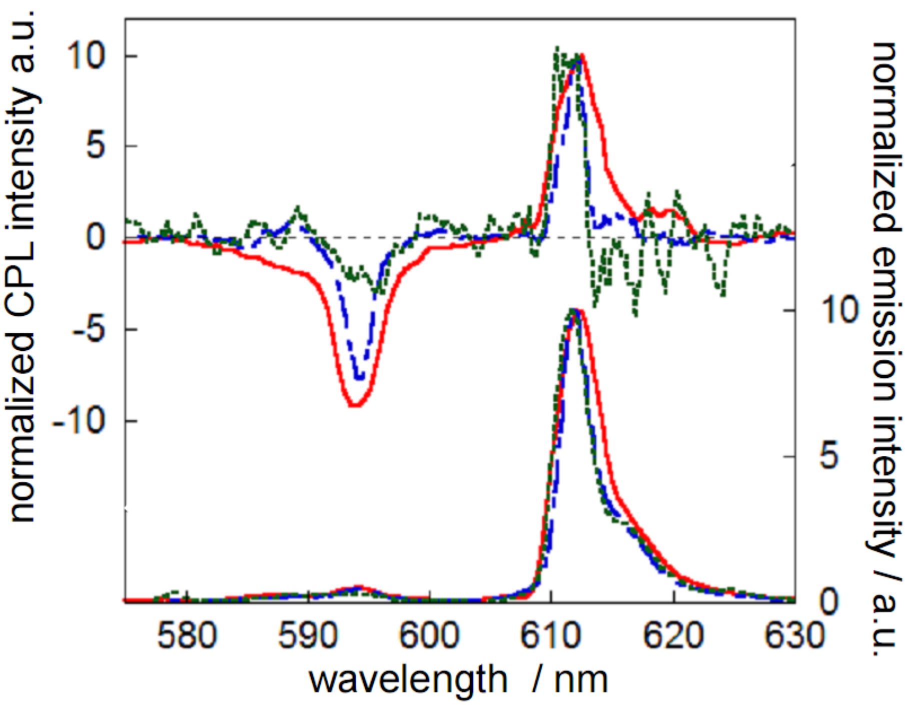

Figure S9. Normalized emission (lower) and CPL-ΔI (upper) spectra of **1-*R*** (red line), **1-*S*** (blue), and **3** (green). Solvents used are acetonitrile-d_3 (> 3.0 mM). All spectra are normalized to the $^5D_0 \rightarrow {}^7F_2$ transition band.

Table S3. Emission quantum yields (Φ_{em})[a], emission lifetimes (τ_{em}), radiative rate constants (k_r), nonradiative rate constants (k_{nr}), relative integrated emission intensities (A_{rel})[b], dissymmetry factor in acetonitrile-d_3

complex	Φ_{em} / %	τ_{em}/ μs	k_r / s^{-1}	k_{nr} / s^{-1}	A_{rel}	g_{ED}	g_{MD}
1-*R*	1.5	160	94	6.2×10^3	19	-0.40	0.029
1-*S*	1.5	160	94	6.2×10^3	20	-0.25	0.016
3	0.29	15 (96%), 150 (4%)			18	-0.17	0.017

[a] Φ_{em} values in acetonitrile-d_3 (1.0 mM) were measured under excitation at 465 nm ($^7F_0 \rightarrow {}^5D_2$, the direct excitation band of Eu(III) ion). τ_{em} values were measured under excitation at 337 nm.

[b] $A_{rel} = A_{5D0\rightarrow7F2} / A_{5D0\rightarrow7F1}$, where $A_{5D0\rightarrow7F2}$ and $A_{5D0\rightarrow7F1}$ are the integrated emission intensities of $^5D_0 \rightarrow {}^7F_2$ and $^5D_0 \rightarrow {}^7F_1$ transition bands.

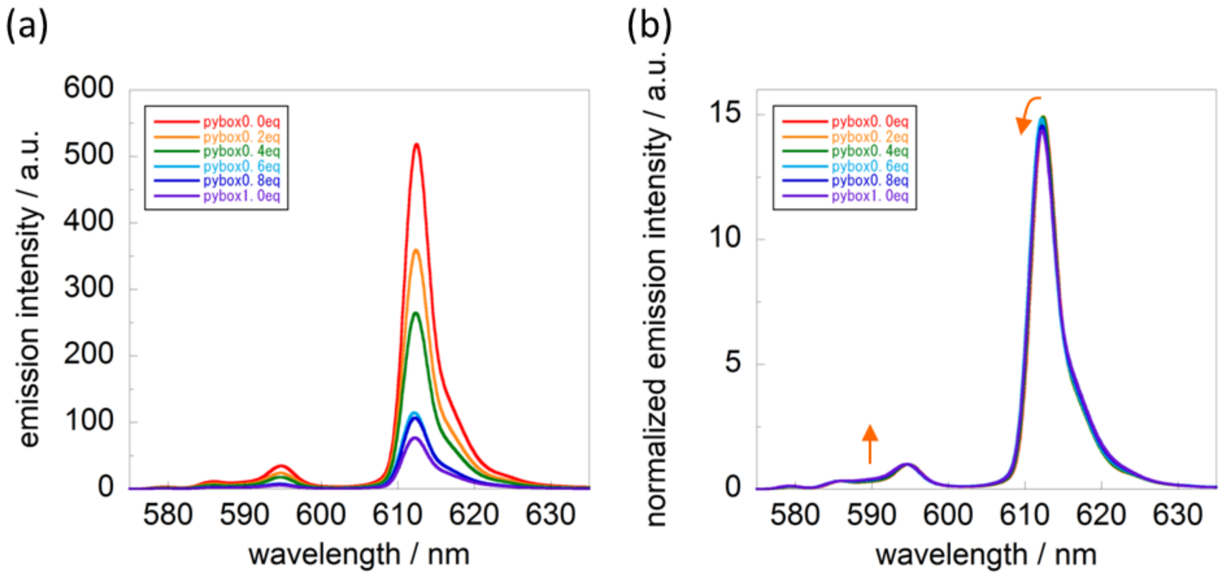

Figure S10. (a) The variant emission intensities of **1-*R*** depend on added *R*-iPr-Pybox ligands. **1-*R*** was dissolved in acetone-d_6 (1.0 mM, not bubbled with N_2 gas). (b) The normalized emission spectra of (a). These spectra were normalized at the maximum intensity of the $^5D_0 \rightarrow {}^7F_1$ transition (ca. 594.5 nm).

Appendix I: Detailed Procedure of Shape Measure Estimations

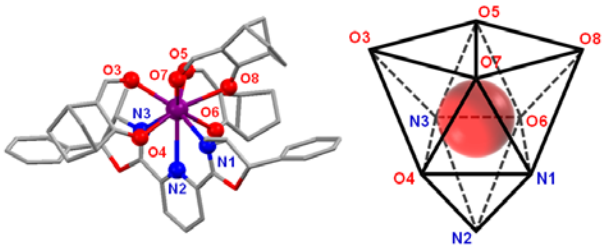

Figure S11. Coordination geometry assignement of **2-*SS*** giving least *S* value. Some atoms are omitted for clarity. Purple; Eu, red; O, blue; N, gray; C.

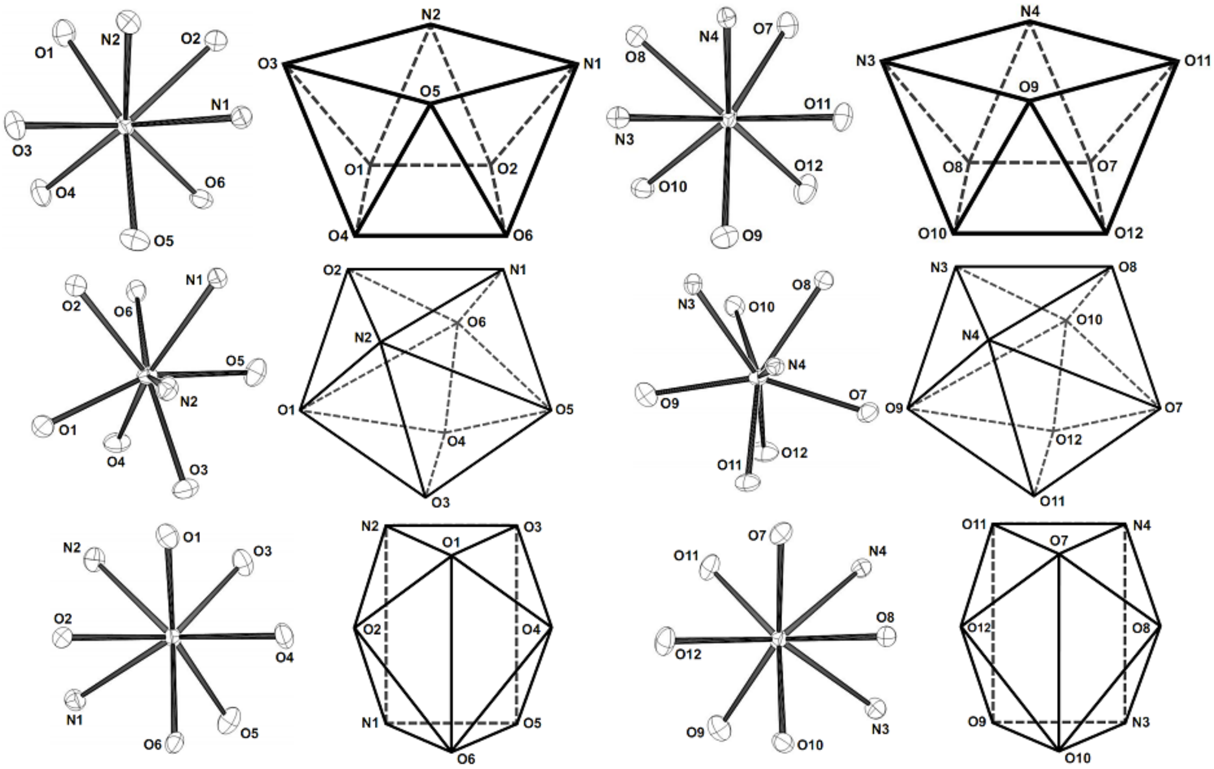

Figure S12. Coordination orientations with the least *S* values for possible geometries of **3**, square antiprism; SAP (top), trigonal dodecahedron; TD (middle), bicapped trigonal prism; BTP (bottom). (for Eu1 site; left, for Eu2 site; right).

Table S4. Shape measure estimations of **1-*R*** for CSAP ($S(C_{4v})$)

	Eu1 site			Eu2 site			Eu3 site		
θ_i	edge	δ_i	$\lvert\delta_i - \theta_i\rvert$	edge	δ_i	$\lvert\delta_i - \theta_i\rvert$	edge	δ_i	$\lvert\delta_i - \theta_i\rvert$
58.88	O5-N3	65.18	6.30	O13-N6	67.28	8.40	O19-N9	68.33	9.45
58.88	O5-O6	57.12	1.76	O13-O14	56.75	2.13	O19-O20	54.21	4.67
58.88	O5-O7	57.31	1.57	O13-O15	59.77	0.89	O19-23	57.55	1.33
58.88	O5-O8	59.72	0.84	O13-O16	58.28	0.60	O19-O24	61.49	2.61
38.31	N3-O6	32.12	6.19	N6-O14	27.06	11.25	N9-O20	62.62	5.69
38.31	O6-O7	42.03	3.72	O14-O15	40.16	1.85	O20-O23	42.94	4.63
38.31	O7-O8	39.65	1.34	O15-O16	38.92	0.61	O23-O24	40.95	2.64
38.31	O8-N3	37.17	1.14	O16-N6	39.54	1.23	O24-N9	31.28	7.03
69.07	N1-N2	67.52	1.55	N4-N5	67.23	1.84	N8-N7	79.68	10.61
69.07	N2-O4	57.43	11.64	N5-O12	55.88	13.19	N7-O21	80.78	11.71
69.07	O4-O3	60.80	8.27	O12-O11	59.43	9.64	O21-O22	69.53	0.46
69.07	O3-N1	69.04	0.03	O11-N4	68.40	0.67	O22-N8	66.77	2.30
52.63	N1-O6	52.07	0.56	N4-O14	53.46	0.83	N9-N8	63.05	10.42
52.63	O6-N2	49.93	2.70	O14-N5	49.36	3.27	N8-O20	47.99	4.64
52.63	N2-N3	62.64	10.01	N5-N6	65.59	12.96	O20-N7	51.84	0.79
52.63	N3-O4	52.53	0.10	N6-O12	49.54	3.09	N7-O23	44.02	8.61
52.63	O4-O8	47.32	5.31	O12-O16	46.79	5.84	O23-O21	53.75	1.12
52.63	O8-O3	57.92	5.29	O16-O11	59.43	6.80	O21-O24	56.75	4.12
52.63	O3-O7	56.50	3.87	O11-O15	58.49	5.86	O24-O22	50.61	2.02
52.63	O7-O1	43.19	9.44	O15-N4	42.31	10.32	O22-N9	53.93	1.30
0.00[a]	N1-O4	14.83	14.83	N4-O12	21.21	21.21	N8-O21	13.20	13.20
	$S(C_{4v})$	**6.15**		**$S(C_{4v})$**	**7.98**		**$S(C_{4v})$**	**6.50**	

[a]The square plane of CSAP was divided into two triangular planes, and the dihedral angle δ_i between two triangular planes was calculated (The θ_i of square plane is zero).

Table S5. Shape measure estimations of **1-*R*** for TTP ($S(D_{3h})$)

	Eu1 site			Eu2 site			Eu3 site		
θ_i	edge	δ_i	$\|\delta_i - \theta_i\|$	edge	δ_i	$\|\delta_i - \theta_i\|$	edge	δ_i	$\|\delta_i - \theta_i\|$
47.49	N1-O6	52.07	4.58	N4-O14	53.46	5.97	N7-O20	51.84	4.35
47.49	O6-O7	42.03	5.46	O14-O15	40.16	7.33	O20-O23	42.94	4.55
47.49	O7-N1	43.19	4.30	O15-N4	42.31	5.18	O23-N7	44.02	3.47
47.49	O4-N3	52.53	5.04	O12-N6	49.54	2.05	O22-N9	53.93	6.44
47.49	N3-O8	37.17	10.32	N6-O16	39.54	7.95	N9-O24	31.28	16.21
47.49	O8-O4	47.32	0.17	O16-O12	46.79	0.70	O24-O22	50.61	3.12
27.40	N1-O4	14.83	12.57	N4-O12	21.21	6.19	N7-O22	11.66	15.74
27.40	O6-N3	32.12	4.72	O14-N6	27.06	0.34	O20-N9	32.62	5.22
27.40	O7-O8	39.65	12.25	O15-O16	38.92	11.52	O23-O24	40.95	13.55
59.38	N2-N1	67.52	8.14	N5-N4	67.23	7.85	N8-N9	63.05	3.67
59.38	N2-N3	62.64	3.26	N5-N6	65.59	6.21	N8-N7	70.56	11.18
59.38	N2-O4	57.43	1.95	N5-O12	55.88	3.50	N8-O20	47.99	11.39
59.38	N2-O6	49.93	9.45	N5-O14	49.36	10.02	N8-O22	58.04	1.34
59.38	O3-N1	69.04	9.66	O11-N4	68.40	9.02	O19-N9	68.33	8.95
59.38	O3-O4	60.80	1.42	O11-O12	59.43	0.05	O19-O20	54.21	5.17
59.38	O3-O7	56.50	2.88	O11-O15	58.46	0.92	O19-O23	57.55	1.83
59.38	O3-O8	57.92	1.46	O11-O16	56.44	2.94	O19-O24	61.49	2.11
59.38	O5-N3	65.68	6.30	O13-N6	67.28	7.90	O21-N9	72.00	12.62
59.38	O5-O6	57.12	2.26	O13-O14	56.75	2.63	O21-O22	60.96	1.58
59.38	O5-O7	57.31	2.07	O13-O15	59.77	0.39	O21-O22	53.75	5.63
59.38	O5-O8	59.72	0.34	O13-O16	58.28	1.10	O21-O24	56.75	2.63
	$\mathbf{S(D_{3h})}$	**6.39**		$\mathbf{S(D_{3h})}$	**5.89**		$\mathbf{S(D_{3h})}$	**8.19**	

Table S6. Shape measure estimations of **1-*S*** for CSAP ($S(C_{4v})$).

	Eu1 site			Eu2 site			Eu3 site			Eu4 site		
θ_i	edge	δ_i	$\|\delta_i - \theta_i\|$	edge	δ_i	$\|\delta_i - \theta_i\|$	edge	δ_i	$\|\delta_i - \theta_i\|$	edge	δ_i	$\|\delta_i - \theta_i\|$
58.88	O3-N1	67.62	8.84	O15-N4	68.90	10.02	O23-N7	67.65	8.77	O27-N10	69.67	10.79
58.88	O3-O4	50.56	8.32	O15-O13	62.62	3.74	O32-O21	88.19	29.31	O27-O29	59.18	0.30
58.88	O3-O6	57.08	1.80	O15-O14	51.57	7.31	O23-O22	58.36	0.52	O27-O30	56.41	2.47
58.88	O3-O5	62.99	4.11	O15-O16	50.37	8.51	O23-O24	58.36	0.52	O27-O28	53.68	5.20
38.31	N1-N4	40.18	1.87	N4-O13	27.54	10.77	N7-O21	35.98	2.33	N10-O28	27.45	10.86
38.31	O4-O6	42.41	4.10	O13-O14	40.49	2.18	O21-O22	40.36	2.05	O28-O30	47.19	8.88
38.31	O6-O5	41.11	2.80	O14-O16	50.13	11.82	O22-O24	43.24	4.93	O30-O29	40.09	1.78
38.31	O5-N1	28.04	10.27	O16-N4	30.85	7.46	O24-N7	28.57	9.74	O29-N10	35.30	3.01
69.07	N2-N3	78.17	9.10	N5-N6	88.87	19.80	N8-N9	68.69	0.38	N11-N12	68.69	0.38
69.07	N3-O8	78.91	9.84	N6-O12	89.96	20.89	N9-O20	70.93	1.86	N12-O32	70.49	1.42
69.07	O8-O7	67.02	2.05	O12-O11	71.37	2.30	O21-O19	59.12	9.95	O32-O31	57.47	11.60
69.07	O7-N2	61.28	7.79	O11-N5	62.59	6.48	O19-N8	53.73	15.34	O31-N11	52.00	17.07
52.63	N1-N2	64.08	11.45	N4-N5	69.93	17.30	N7-N8	65.64	13.01	N10-N11	66.86	14.23
52.63	N2-O4	78.17	25.54	N5-O16	51.71	0.92	N8-O24	51.73	0.90	N11-O28	51.44	1.19
52.63	O4-N3	47.52	5.11	O16-N6	45.67	6.96	O24-N9	50.38	2.25	O28-N12	49.75	2.88
52.63	N3-O6	46.83	5.80	N6-O14	40.02	12.61	N9-O22	41.67	10.96	N12-O30	40.82	11.81
52.63	O6-O8	52.29	0.34	O14-O12	54.41	1.78	O22-O20	56.66	4.03	O30-O32	56.43	3.80
52.63	O8-O5	57.43	4.80	O12-O13	56.75	4.12	O20-O21	56.57	3.94	O32-O29	57.36	4.73
52.63	O5-O7	52.37	0.26	O13-O11	53.78	1.15	O21-O19	48.72	3.91	O29-O31	47.31	5.32
52.63	O7-N1	56.19	3.56	O11-N4	57.35	4.72	O19-N7	53.34	0.71	O31-N10	57.31	4.68
0.00[a]	N3-O7	6.32	6.32	N6-O11	18.72	18.72	N9-O19	18.44	18.44	N12-O31	21.06	21.06
	$S(C_{4v})$	**8.34**		**$S(C_{4v})$**	**9.86**		**$S(C_{4v})$**	**9.97**		**$S(C_{4v})$**	**8.91**	

[a]The square plane of CSAP was divided into two triangular planes, and the dihedral angle δ_i between two triangular planes was calculated (The θ_i of square plane is zero).

Table S7. Shape measure estimations of **1-*S*** for TTP ($S(D_{3h})$).

	Eu1 site			Eu2 site			Eu3 site			Eu4 site		
θ_i	edge	δ_i	$\lvert\delta_i - \theta_i\rvert$	edge	δ_i	$\lvert\delta_i - \theta_i\rvert$	edge	δ_i	$\lvert\delta_i - \theta_i\rvert$	edge	δ_i	$\lvert\delta_i - \theta_i\rvert$
47.49	N1-O5	28.04	19.45	N4-O11	57.35	9.86	N7-O19	53.34	5.85	N10-O29	35.30	12.19
47.49	O5-O7	52.37	4.88	O11-O13	53.78	6.29	O19-O21	48.72	1.23	O29-O31	47.31	0.18
47.49	O7-N1	56.19	8.70	O13-N4	27.54	19.95	O21-N7	35.98	11.51	O31-N10	53.71	6.22
47.49	O4-O6	42.41	5.08	O16-N6	45.67	1.82	O24-N9	50.38	2.89	O28-O30	47.19	0.30
47.49	O6-N3	46.48	1.01	N6-O14	40.02	7.47	N9-O22	41.67	5.82	O30-N12	40.82	6.67
47.49	N3-O4	47.52	0.03	O14-O16	50.13	2.64	O22-O24	43.24	4.25	N12-O28	49.75	2.26
27.40	N1-O4	40.18	12.78	N4-O16	30.85	3.45	N7-O24	28.57	1.17	N10-O28	27.45	0.05
27.40	O5-O6	41.11	13.71	O11-N6	18.72	8.68	O19-N9	18.44	8.96	O29-O30	40.09	12.69
27.40	O7-N3	6.32	21.08	O13-O14	40.49	13.09	O21-O22	40.36	12.96	O31-N12	21.06	6.34
59.38	N2-N1	64.08	4.70	N5-N4	69.93	10.55	N8-N7	65.64	6.26	N11-N10	66.86	7.48
59.38	N2-N3	73.24	13.86	N5-N6	73.90	14.52	N8-N9	68.69	9.31	N11-N12	68.69	9.31
59.38	N2-O4	46.75	12.63	N5-O11	48.70	10.68	N8-O19	53.73	5.65	N11-O28	51.44	7.94
59.38	N2-O7	56.67	2.71	N5-O16	51.71	7.67	N8-O24	51.73	7.65	N11-O31	52.00	7.38
59.38	O3-N1	67.72	8.34	O12-N6	73.71	14.33	O20-N9	70.93	11.55	O27-N10	69.67	10.29
59.38	O3-O4	50.56	8.82	O12-O11	57.99	1.39	O20-O19	59.12	-0.26	O27-O28	53.68	5.70
59.38	O3-O5	62.99	3.61	O12-O13	56.75	2.63	O20-O21	56.57	2.81	O27-O29	59.18	0.20
59.38	O3-O6	57.08	2.30	O12-O14	54.41	4.97	O20-O22	56.66	2.72	O27-O30	56.41	2.97
59.38	O8-N3	73.95	14.57	O15-N4	68.90	9.52	O23-N7	67.65	8.27	O32-N12	70.49	11.11
59.38	O8-O5	57.45	1.93	O15-O13	62.62	3.24	O23-O21	58.36	1.02	O32-O29	57.36	2.02
59.38	O8-O6	52.29	7.09	O15-O14	51.37	8.01	O23-O22	58.36	1.02	O32-O30	56.43	2.95
59.38	O8-O7	62.44	3.06	O15-O16	50.37	9.01	O23-O24	54.52	4.86	O32-O31	57.47	1.91
	$S(D_{3h})$	**10.05**		**$S(D_{3h})$**	**9.36**		**$S(D_{3h})$**	**6.68**		**$S(D_{3h})$**	**6.85**	

Table S8. Shape measure estimations of **2-*SS*** for CSAP ($S(C_{4v})$) and TTP ($S(D_{3h})$).

CSAP				TTP			
θ_i	edge	δ_i	$\|\delta_i - \theta_i\|$	θ_i	edge	δ_i	$\|\delta_i - \theta_i\|$
58.88	N2-N1	62.37	3.49	47.49	N1-O4	46.21	1.28
58.88	N2-O4	49.27	-9.61	47.49	O4-O7	46.93	0.56
58.88	N2-N3	67.61	8.73	47.49	O7-N1	47.90	0.41
58.88	N2-O6	56.70	2.18	47.49	O6-N3	34.25	13.24
38.31	N1-O4	46.21	7.90	47.49	N3-O5	52.75	5.26
38.31	O4-N3	35.09	3.22	47.49	O5-O6	47.60	0.11
38.31	N3-O6	34.25	4.06	27.40	N1-O6	27.72	0.32
38.31	O6-N1	27.72	10.59	27.40	O4-N3	35.09	7.69
69.07	O3-O5	62.27	6.80	27.40	O7-O5	19.44	7.96
69.07	O5-O8	65.15	3.92	59.38	N2-N1	62.37	2.99
69.07	O8-O7	67.20	1.87	59.38	N2-N3	67.61	8.23
69.07	O7-O3	67.14	1.93	59.38	N2-O4	49.27	10.11
52.63	N1-O7	47.90	4.73	59.38	N2-O6	56.70	2.68
52.63	O7-O4	46.93	5.70	59.38	O3-N3	61.37	1.99
52.63	O4-O3	52.16	0.47	59.38	O3-O4	52.16	7.22
52.63	O3-N3	61.37	8.74	59.38	O3-O5	62.27	2.89
52.63	N3-O5	52.75	0.12	59.38	O3-O7	67.14	7.76
52.63	O5-O6	47.60	5.03	59.38	O8-N1	57.52	1.86
52.63	O6-O8	54.77	2.14	59.38	O8-O5	65.15	5.77
52.63	O8-N1	57.52	4.89	59.38	O8-O6	54.77	4.61
0.00	O5-O7	19.44	19.44	59.38	O8-O7	67.20	7.82
	$S(C_{4v})$	**6.97**			**$S(D_{3h})$**	**6.01**	

Table S9. Shape measure estimations of **3** for SAP ($S(C_{4v})$), TTP ($S(D_{3h})$).

	SAP						TTP						
	Eu1 site			Eu2 site				Eu1 site			Eu2 site		
θ_i	edge	δ_i	$\lvert\delta_i - \theta_i\rvert$	edge	δ_i	$\lvert\delta_i - \theta_i\rvert$	θ_i	edge	δ_i	$\lvert\delta_i - \theta_i\rvert$	edge	δ_i	$\lvert\delta_i - \theta_i\rvert$
0.00	N2 – O5	7.26	7.26	N4 – O9	4.94	4.94	29.86	N2-O1	51.58	21.72	N4-O9	4.94	24.92
0.00	O1 – O6	9.12	9.12	O8 – O12	9.07	9.07	29.86	N2-O5	7.26	22.60	N3-O7	51.80	21.94
77.1	N1 – O5	74.01	3.09	N3 – N4	83.96	6.86	29.86	O1-O6	9.12	20.74	O9-O10	53.73	23.87
77.1	O5 – O3	64.71	12.39	N4 – O11	78.62	1.52	29.86	O5-O6	56.03	26.17	O7-O10	8.57	21.29
77.1	O3 – N2	79.26	2.16	O11 – O9	63.07	14.03	53.12	N1-O2	58.45	5.33	N3-O8	53.76	0.64
77.1	N2 – N1	80.65	3.55	O9 – N3	74.97	2.13	53.12	O3-O4	62.18	9.06	O11-O12	59.89	6.77
77.1	O2 – O6	70.95	6.15	O8 – O7	80.31	3.21	53.12	N1-O6	45.23	16.25	N3-N4	83.96	22.48
77.1	O6 – O4	77.10	0.00	O7 – O12	79.31	2.21	53.12	O2-O6	70.95	9.47	N4-O8	45.24	16.24
77.1	O4 – O1	74.49	2.61	O12 – O10	80.55	3.45	61.48	N1-N2	80.65	19.17	N3-O10	47.77	13.71
77.1	O1 – O2	80.76	3.66	O10 – O8	78.94	1.84	61.48	N2-O2	44.19	17.29	O8-O10	72.49	11.01
51.6	N1 – O6	45.23	6.37	N3 – O8	53.76	2.16	61.48	O1-O4	74.49	13.01	O9-O12	55.46	6.02
51.6	O6 – O5	56.03	4.43	O8 – N4	45.24	6.36	61.48	O1-O3	44.88	16.60	O9-O11	63.07	1.59
51.6	O5 – O4	50.19	1.41	N4 – O7	51.80	0.20	61.48	O3-O5	64.71	3.23	O7-O12	73.22	11.74
51.6	O4 – O5	62.18	10.58	O7 – O11	48.81	2.79	61.48	O4-O5	50.19	11.29	O7-O11	48.81	12.67
51.6	O3 – O1	44.88	6.72	O11 – O12	59.89	8.29	74.29	O1-O2	73.97	0.32	N3-O9	74.97	0.68
51.6	O1 – N2	51.58	0.02	O12 – O9	55.46	3.86	74.29	N1-O5	74.01	0.28	O7-O8	73.93	0.36
51.6	N2 – O2	44.19	7.41	O9 – O10	53.73	2.13	74.29	O4-O6	77.10	2.81	N4-O11	78.62	4.33
51.6	O2 – N1	58.45	6.85	O10 – N3	47.77	3.83	74.29	N2-O3	79.26	4.97	O10-O12	74.51	0.22
	$S(D_{4d})$	**6.22**		**$S(D_{4d})$**	**5.50**			**$S(D_{2d})$**	**14.61**		**$S(D_{2d})$**	**14.15**	

Table S10. Shape measure estimations of **3** for BTP ($S(C_{2v})$).

	Eu1 site			Eu2 site		
θ_i	edge	δ_i	$\lvert\delta_i - \theta_i\rvert$	edge	δ_i	$\lvert\delta_i - \theta_i\rvert$
0.0	N2 – O5	7.26	7.26	N4 – O9	4.94	4.94
18.0	O1 – O6	9.12	8.88	O7 – O10	8.57	9.43
46.3	N1 – O6	45.23	1.07	N3 – O10	47.77	1.47
46.3	N2 – O1	51.58	5.28	N4 – O7	51.80	5.50
46.3	O1 – O3	44.88	1.42	O7 – O10	48.81	2.51
46.3	O5 – O6	56.03	9.73	O9 – O10	53.73	7.43
62.2	N1 – N2	80.65	18.45	N3 – N4	83.96	21.76
62.2	O3 – O5	64.71	2.51	O9 – O11	63.07	0.87
69.2	N1 – O2	58.45	10.75	N3 – O8	53.76	15.44
69.2	N2 – O2	44.19	25.01	N4 – O8	45.24	23.96
69.2	O3 – O4	62.18	7.02	O9 – O12	55.46	13.74
69.2	O4 – O5	50.19	19.01	O11 – O12	59.89	9.31
88.7	N1 – O5	74.01	14.69	N3 – O9	74.97	13.73
88.7	N2 – O3	79.26	9.44	N4 – O11	78.62	10.08
64.2	O1 – O2	73.97	9.77	O7 – O8	73.93	9.73
64.2	O1 – O4	74.49	10.29	O7 – O12	73.22	9.02
64.2	O2 – O6	70.95	6.75	O8 – O10	72.49	8.29
64.2	O4 – O6	77.10	12.90	O10 – O12	74.51	10.31
	$S(C_{2v})$	**11.72**		**$S(C_{2v})$**	**11.57**	

The ideal nona-coordinated structures by using mathematical calculation for shape measure estimations of nona-coordinated structures. Mathematical calculations were performed by using GNU OCTAVE 2.1.50 software.

The calculation model of ideal capped square antiprism (CSAP). Before calculations, we modeled the ideal CSAP structure, as follows,

(1) The centered metal called, *M* is placed at the center of a sphere of radius of 1. The coordinate of *M* is expressed as *M*(0, 0, 0) in the x-y-z space. All the coordinated atoms are placed on the sphere.

(2) The principal axis of CSAP is along with z axis. The capped atom called as *A* is thus located at *A*(0, 0, 1).

(3) Two square planes, *square1* and *square2* are fixed perpendicular to the principal axis. *Square1* is closer to *A* compared with *square 2*. We assume here that square1 is located on *z* = b, and *square2* on the *z* = d. The relation between b and d are 1 > b > d > -1, respectively. *Square2* was twisted by 45 degree from *square1*.

(4) Four vertices of *square1* called as *B*, *C*, *D*, and *E*, are located on *B*(a, 0, b), *C*(0, a, b), *D*(-a, 0, b), and *E*(0, -a, b), where a > 0 and $a^2 + b^2 = 1$ from the Pythagorean theorem. In a similar way, four vertices of *square2*, *F*, *G*, *H*, and *I* are on *F*(c, c, d), *G*(-c, c, d), *H*(-c, -c, d) and *I*(c, -c, d), where c > 0 and $2c^2 + d^2 = 1$.

After locating nine atoms, the sum of the atom-atom distances were calculated with various b and d values within the condition, 1 > b > d > -1. The repulsion energy between atom-atom decreases when the atom-atom distance increases. In this calculation, the largest sum of the atom-atom distances with the smallest repulsion energy was determined, where b and d were found to be 0.3628 and -0.6130, respectively.

The calculation of ideal tricapped trigonal prism (TTP). The assumptions of ideal TTP are listed as below.

(1) The centered metal *M* is at (0, 0, 0), and the all coordinated atoms are on a sphere with radius of 1, just as the case of CSAP.

(2) We consider a trigonal prism which was constructed by the two regular triangle planes, Δ*ABC* and Δ*DEF*. The center of gravity of this prism are *M*(0, 0, 0). ΔABC and ΔDEF are on *z* = b and *z* = -b, where 1 > b > 0. *A* and *D* are on the x axis.

(3) We consider that three tricapped atoms called as *G*, *H*, and *I* can create the regular triangle plane, Δ*GHI*. Δ*GHI* crosses the trigonal prism and are on the *xy* plane (*z* = 0). *G*, *H* and *I* atoms are located as *AH*, *BG* and *CI* cross perpendicularly the square planes *BCEF*, *ACDF*, and *ABDE*, respectively.

After locating nine atoms, the sum of the atom-atom distances were calculated with various b within the condition, 1 > b > 0. In this calculation, the largest sum of the atom-atom distances with the smallest repulsion energy was determined, where b was found to be 0.7031. All the Cartesian coordinates of nine atoms constructing CSAP and TTP were listed in Table S9.

Table S11. The Cartesian Coordinates of Atoms Constructing Ideal CSAP (left) and TTP (right) Structures

	CSAP			TTP		
Atoms	X	Y	Z	X	Y	Z
A	0	0	1	0.7111	0	0.7031
B	0.9319	0	0.3628	-0.3556	-0.6158	0.7031
C	0	0.9319	0.3628	-0.3556	0.6158	0.7031
D	-0.9319	0	0.3628	0.7111	0	-0.7031
E	0	-0.9319	0.3628	-0.3156	-0.6158	-0.7031
F	0.5587	0.5587	-0.6130	-0.3156	0.6158	-0.7031
G	-0.5587	0.5587	-0.6130	-0.5	0.8660	0
H	-0.5587	-0.5587	-0.6130	-1.0	-0	0
I	0.5587	-0.5587	-0.6130	0.5	0.8660	0

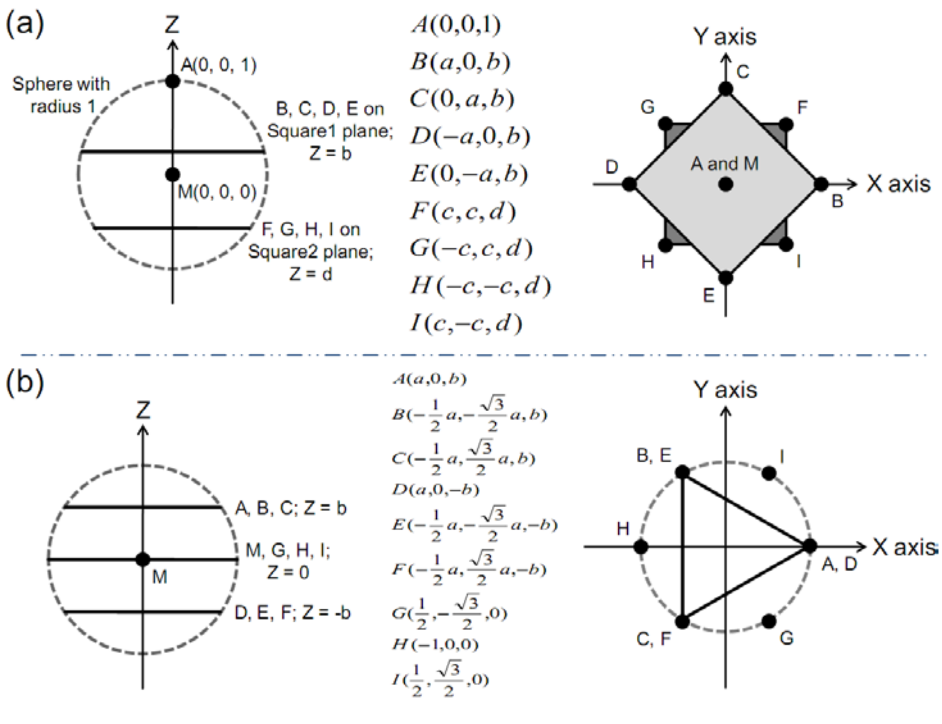

Figure S13. Ideal (a) CSAP and (b) TTP models and coordinates.

Calculation procedure;

(1) **Ideal CSAP**

Distances of all the edges of CSAP:

AB/AC/AD/AE: $f = \sqrt{2(1-b)}$

AF/AG/AH/AI: $g = \sqrt{2(1-d)}$

BC/CD/DE/EB: $h = \sqrt{2(1-b^2)}$

FG/GH/HI/IF: $j = 2\sqrt{\frac{1-d^2}{2}}$

BC/CE: $k = 2\sqrt{1-b^2}$

FH/GI: $l = 2\sqrt{1-d^2}$

BF/FC/CG/GD/DH/HE/EI/IB: $m = \sqrt{2-\sqrt{2(1-b^2-d^2+b^2d^2)}-2bd}$

BG/BH/CH/CI/DF/DI/EF/EG: $n = \sqrt{2+\sqrt{2(1-b^2-d^2+b^2d^2)}-2bd}$

The sum of distances; $o = 4f + 4g + 4h + 4j + 2k + 2l + 8m + 8n$ (36 edges)

```
#[GNU Octave 2.1.50]
for b=0.99:-0.01:-0.98
for d=(b-0.01):-0.01:-0.99
f=sqrt(2-2*b);
g=sqrt(2-2*d);
h=sqrt(2-2*b*b);
j=2*sqrt((1-d*d)/2);
k=sqrt(2-sqrt(2-2*d*d-2*b*b+2*b*b*d*d)-2*b*d);
l=2*sqrt(1-b*b);
m=2*sqrt(1-d*d);
n=sqrt(2+sqrt(2-2*d*d-2*b*b+2*b*b*d*d)-2*b*d);
o=(4*f)+(4*g)+(4*h)+(4*j)+(8*k)+(2*l)+(2*m)+(8*n);
disp(b), disp(o)
end      (end loop for d)
end      (end loop for b)
```

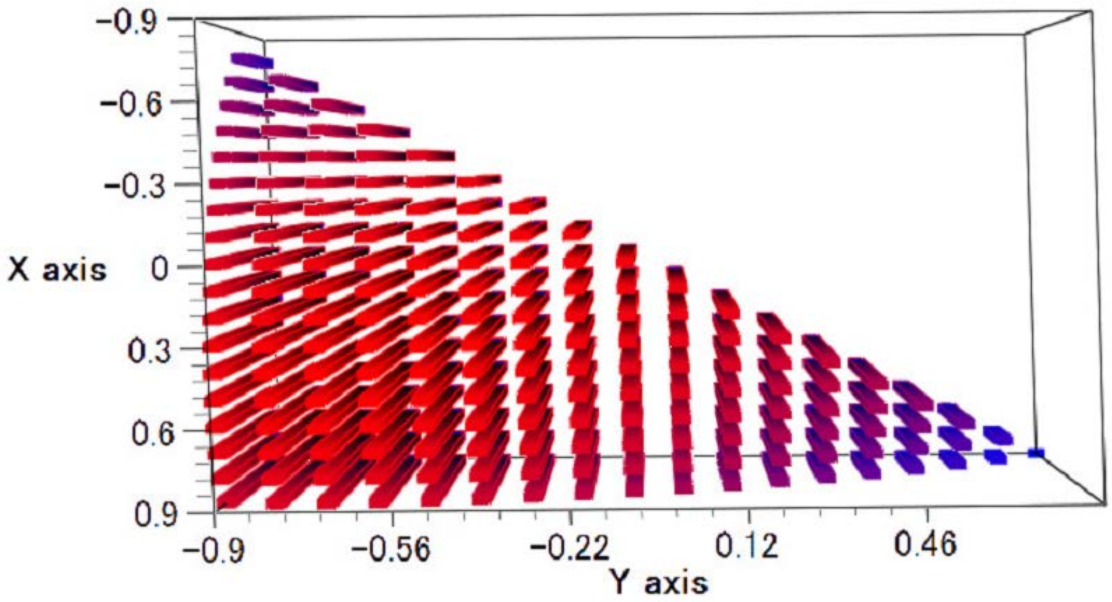

Figure S14. o values with various b and d values (x axis; b, y axis; d)

The dihedral angles, θ_i were calculated by using the obtained coordinates.

AB/AC/AD/AE: 58.88 deg

BC/BE/CD/DE: 38.31 deg

FG/FI/GH/HI: 69.07 deg

BF/BI/CF/CG/DG/DH/EH/EI: 52.63 deg

(In order to perform the shape measure estimations, we needed to divide the square “FGHI” into two triangle, “ΔFGH/ΔFHI” or “ΔFGI/ΔFHI” and calculate the dihedral angels between these two triangular planes.)

(2) **Ideal TTP.**

Distances of all the edges of TTP:

AB/AC/BC/DE/DF/EF: $X1 = \sqrt{3(1-b^2)}$

AD/BE/CF: $X2 = 2b$

AG/AI/BG/BH/CH/CI/DG/DI/EG/EH/FH/FI: $X3 = \sqrt{2-\sqrt{1-b^2}}$

AE/AF/BD/BF/CD/CE: $X4 = \sqrt{3+b^2}$

AH/BI/CG/DH/EI/FG: $X5 = \sqrt{2+2\sqrt{1-b^2}}$

GH/GI/GH: $X6 = \sqrt{3}$

The sum of distances; $X7 = 6\times X1 + 3\times X2 + 12\times X3 + 6\times X4 + 6\times X5 + 3\times X6$ (36 edges)

```
#[GNU Octave 2.1.50]
format long
for b=0.01:0.01:0.99
X1=sqrt(3-3*b*b);
X2=2*b;
X3=sqrt(2-sqrt(1-b*b));
X4=sqrt(3+b*b);
X5=sqrt(2+2*sqrt(1-b*b));
X6=sqrt(3);
X7=(6*X1)+(3*X2)+(12*X3)+(6*X4)+(6*X5)+(3*X6);
disp(b)
disp(X7)
end
```

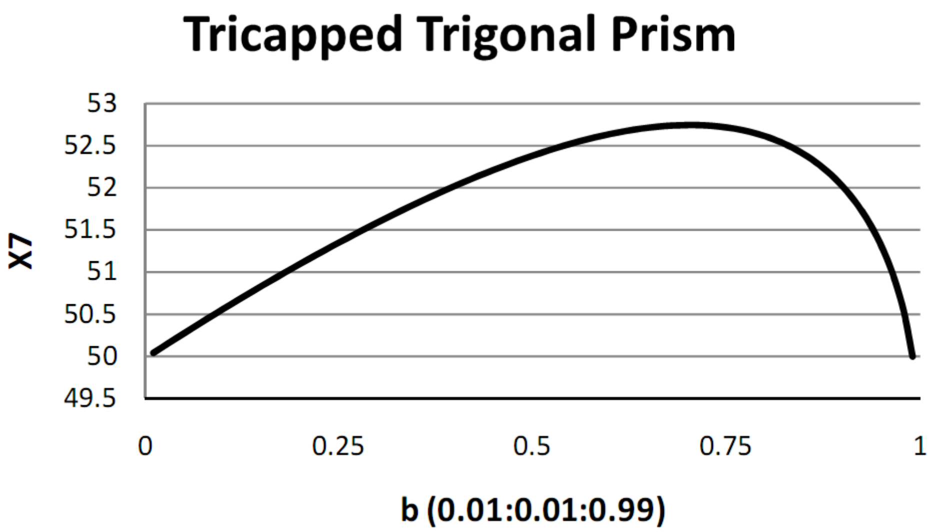

Figure S15. X7 with various b values (x axis; b, y axis; X7)

The dihedral angles, θ_i were calculated by using the obtained coordinates.

AB/AC/BC/DE/DF/EF: 47.49 deg

AD/BE/CF: 27.40 deg

AG/AI/BG/BH/CH/CIDG/DI/EG/EH/FH/FI: 59.38 deg